First simultaneous measurements of peroxyacetyl nitrate (PAN) and ozone at Nam Co in the central Tibetan Plateau: impacts from the PBL evolution and transport processes

Xiaobin Xu[1], Hualong Zhang[1,*], Weili Lin[1,2], Ying Wang[1], and Shihui Jia[1,]**

[1]{State Key Laboratory of Severe Weather & Key Laboratory for Atmospheric Chemistry of China Meteorological Administration, Chinese Academy of Meteorological Sciences, Beijing, China}

[2]{Meteorological Observation Center, China Meteorological Administration, Beijing, China}

[*]{now at : Guangdong Meteorological Observatory, Guangzhou, Guangdong, China}

[**]{now at: School of Environment and Energy, South China University of Technology, Guangzhou, Guangdong, China}

Correspondence to: Xiaobin Xu (xuxb@camscma.cn)

Abstract

Both peroxyacetyl nitrate (PAN) and ozone (O_3) are key photochemical products in the atmosphere. Most of the previous in-situ observations of both gases have been made in polluted regions and at low altitude sites. Here we present first simultaneous measurements of PAN and O_3 at Nam Co (NMC, 90 °57′E, 30 °46′N, 4745 m a.s.l.), a remote site in the central Tibetan Plateau (TP). The observations were made during summer periods in 2011 and 2012. The PAN concentrations averaged 0.36 ppb (range: 0.11-0.76 ppb) and 0.44 ppb (range: 0.21-0.99 ppb) during 16-25 August 2011 and 15 May to 13 July 2012, respectively. The O_3 concentration varied from 27.9 ppb to 96.4 ppb, with an average of 60.0 ppb. Profound diurnal cycles of PAN and O_3 were observed, with minimum values around 5:00 LT, steep rises in the early morning, and broader platforms of high values during 9:00-20:00 LT. We find that the evolution of planetary boundary layer (PBL) played a key role in shaping the diurnal patterns of both gases, particularly the rapid increases of PAN and O_3 in the early

morning. Air entrainment from the free troposphere into the PBL seemed to cause the early morning increase and be a key factor of sustaining the daytime high concentrations of both gases. The days with higher daytime PBL (about 3 km) showed stronger diurnal variations of both gases and were mainly distributed in the drier pre-monsoon period, while those with shallower daytime PBL (about 2 km) showed minor diurnal variations of both gases and were mainly distributed in the humid monsoon period. Episodes of higher PAN levels were observed occasionally at NMC. These PAN episodes were caused either by rapid downward transport of air masses from the middle/upper troposphere or by long-range transport of PAN plumes from North India. The PAN level in the downward transport cases ranged from 0.5 ppb to 0.7 ppb and may indicate the PAN abundance in the middle/upper troposphere. In the long-range transport case, the PAN level varied in the range of 0.6-1.0 ppb. This long-range transport process influenced most of the western and central TP region for about a week in early June 2012. Our results suggest that polluted air masses from South Asia can significantly enhance the PAN level over the TP. As PAN act as a reservoir of NO_x, the impacts of pollution transport from South Asia on tropospheric photochemistry over the TP region deserve further studies.

1 Introduction

Peroxyacetyl nitrate (PAN) and ozone (O_3) are important oxidants in the troposphere. They are toxic for human and vegetation. Tropospheric O_3 contributes significantly to global warming with a radiative forcing of +40 (± 0.20) W/m2 (Myhre et al., 2013). Tropospheric O_3 originates mainly from the photochemical reactions within the troposphere and to a lesser extent from the stratosphere (Lelieveld and Dentener, 2000), while PAN in the troposphere is nearly exclusively formed in oxidation of volatile organic compounds (VOCs) in the presence of NO_x (Fischer et al., 2014). PAN is produced in the association reaction between $CH_3C(O)O_2$ (PA) and NO_2. As one of the key radicals, PA is produced by oxidation of a number of VOCs (Roberts, 2007; LaFranchi et al., 2009; Fischer et al., 2014). Since both VOCs and NO_x are largely emitted by anthropogenic sources, PAN is primarily produced in and downwind of industrial and populated areas. With different lifetimes at different temperatures (Cox and Roffey, 1977), PAN is instable under warm conditions, but stays longer in colder environment, thus is revealed ubiquitous in the mid to upper troposphere (Singh, 1987; Talbot et al., 1999; Russo et al., 2003), ultimately resulting in a global scale

1   transport. PAN can decompose and release NO_2 when it reaches warm environment,

2   becoming one of the key sources of NO_x in remote areas. This makes PAN an important

3   reservoir of NO_2. Inter-comparisons among models and between model and observation show

4   very large PAN differences in many regions of the atmosphere (Thakur et al., 1999; Sudo et

5   al., 2002; von Kuhlmann et al., 2003; Singh et al., 2007), but confirm the important role for

6   PAN in sustaining O_3 production over remote regions (Hudman et al., 2004; Zhang et al.,

7   2008). Since tropospheric O_3 and OH are principally controlled by the abundance of NO_x,

8   decomposition of PAN would have great implications for the budget of these key atmospheric

9   oxidants. It has been indicated that regional increase of O_3 can be attributed to an

10   intercontinental and even global transport of PAN (Hudman et al., 2004; Fischer et al., 2011)

11   and most of the conveying paths are in the free troposphere, driving PAN plumes travelling to

12   remote areas (Roiger et al., 2011;Pandey Deolal et al., 2013). Thus a considerable amount

13   of PAN has been detected in remote areas with sparse anthropogenic emission (Zanis, 2007).

14   Up to now the main methods to directly obtain the PAN concentration are ground-based and

15   aircraft observations. Although PAN has been measured in a great deal of campaigns during

16   past decades, the observational data of PAN are very inhomogeneously distributed over the

17   world, with most of them being from North America, West Europe, and Pacific region

18   (Fischer et al., 2014). PAN measurements are extremely lacking in many areas over Eurasian

19   continent, northeastern African, Oceanic regions, the Indian Ocean, and the Tibetan Plateau

20   (TP) region.

21   The TP region covers an area of about 2,500,000 km^2, with an average elevation of about

22   4000 m above sea level. The world's highest plateau acts as a heat core in summer, heating

23   the air above and prompting its ascending motion (Yeh et al., 1957). In addition to the thermal

24   effect, the South Asian monsoon also exerts a convergence effect driving the ascending

25   motion (Chen et al., 2012). Accompanied by the ascending motion, water vapor and air

26   pollutants emitted or formed in the boundary layer can be rapidly transported to the upper

27   troposphere and lower stratosphere (UTLS) (Dessler and Sherwood, 2004; Gettelman and

28   Kinnison, 2004, Fu et al., 2006; Lelieveld et al., 2007; Law et al., 2010). Convective transport

29   over the TP and surrounding areas can be clearly tracked by satellite observations of some

30   longer-lived species, such as CO (Park et al., 2007, 2009), PAN (Ungermann et al., 2016),

31   CH_4 (Xiong et al., 2009) and HCN (Randel et al., 2010). Elevated concentrations of some

32   relatively short-lived anthropogenic pollutants in the UTLS region are also reported (Park et

1   al., 2008, Tian et al., 2008; Gu et al., 2016). Such rapid, upward transport of pollutants and

2   water vapor may have great implications on atmospheric composition and climate of regional

3   and global scales. Efforts have been made to understand the impacts of upward transport of

4   air masses over the TP, among which is the potential relationship with the ozone valley over

5   the TP reported by Zhou et al. (1995).

6   The TP region is very sparsely populated with nearly no industrial emissions of pollutants.

7   Although the TP has been nearly unpolluted, the high altitude and the correspondingly

8   intensified UV radiation make it an interesting region for studies of photochemical products,

9   such as O_3 and PAN. However, there have been only sparse reports of measurements of O_3

10   and related species from the TP mainly due to the poor accessibility and logistic difficulties of

11   this vast region. So far, most of the published measurements of O_3 and its precursors over the

12   TP have been from sites at the edges of the TP (Ma et al., 2002a, 2002b; Ding and Wang,

13   2006; Wang et al., 2006; Zhu et al., 2006; Cristofanelli et al., 2010; Xue et al., 2011; Zheng et

14   al., 2011; Ma et al., 2014; Wang et al., 2015b; Xu et al., 2016, 2017). Only three publications

15   present measurements of O_3 and related species from sites in the central TP, with one

16   reporting data from urban observations (Ran et al., 2014) and two showing results from

17   remote sites (Lin et al., 2015; Yin et al., 2017).

18   Observational data of PAN from the TP are extremely lacking. The only field observation of

19   ambient PAN in the TP was made by Xue et al. (2011), who measured PAN and other

20   reactive species at Mt. Waliguan, a global atmosphere watch (GAW) station located at the

21   northeast edge of the TP. The average level of PAN was 0.44 ($\pm$0.14) ppb for a two-week

22   period in summer 2006. This observation offers a preliminary detection of ambient PAN over

23   the northeast TP. So far, there has been no published in-situ measurement of PAN from the

24   central TP. In addition to the traditional observation methods, remote sensing techniques can

25   also be applied to acquire the global PAN distribution from satellites (Remedios et al., 2007;

26   Moore and Remedios, 2010; Wiegele et al., 2012; Tereszchuk et al., 2013; Fadnavis et al.,

27   2014). However, the PAN data retrieved from satellite observations need further validations.

28   Here we present the first simultaneous measurements of PAN and O_3 at a site in the central

29   TP. We study the diurnal variations of observed concentrations and the links to the evolution

30   of planetary boundary layer (PBL). We also investigate the vertical and horizontal transport

31   and discuss the implications of our measurements.

2   Observations

2.1   Site

The observations of PAN and other species were made from 11 July to 31 August 2011 and from 15 May to 13 July 2012 at the Nam Co Comprehensive Observation and Research Station, Chinese Academy of Sciences (CAS) (NMC, 90 57′E, 30 46′N, 4730 m a.s.l.). West and north of the NMC site is the Nam Co Lake, with the nearest distance to the lake being about 1.5 km. The Nyainqentanglha mountains (about 5000-6800 m a.s.l.) stand south and east of the site, with the mountain ridge being more than 20 km distant from the site. The TP region has a population density of less than 2 person/km^2 (http://sedac.ciesin.columbia.edu/gpw/). The largest city of Tibet, Lhasa, is about 120 km south from the NMC site, far beyond the continuous ridges of the Nyainqentanglha Mountains. The nearest population center, Dangxiong township is located about 35 km southeast of the NMC site. The direct transport of air pollutants from Lhasa and Dangxiong is hardly possible due to the blocking of the high mountain ridges. There is a road about 1.3 km southeast of the NMC site, connecting the tourism site of the Nam Co Lake to Dangxiong and the No. 109 National Road. More details about NMC and its surrounding can be found in literature (Ma et al., 2011; Lin et al., 2015; Yin et al. 2017).

2.2   Instruments and data correction

Ambient PAN was observed using a PAN analyzer (Meteorologie Consult GmbH, Germany), which consists of an automated gas chromatograph (GC) equipped with an electron capture detector (ECD) and a calibration unit. The equipment is the same one used in previous observation in Beijing (Zhang et al., 2014), with identical setup details depicted in the paper. In respect of the calibration system, an NO reference gas (4.5 ppm) in nitrogen was introduced in and reacts with acetone vapor under the UV irradiation. Under the same condition, the PAN standard is produced with the efficiency of 93%$\pm$7% (Volz-Thomas et al., 2002). Surface O_3 was simultaneously observed using an O_3 analyzer (TE 49C, Thermo Environmental Instruments, Inc., USA), which was regularly calibrated using an O_3 calibrator (TE 49C PS) traceable to the Standard Reference Photometer (SRP) maintained by WMO World Calibration Centre in EMPA, Switzerland. All instruments were housed in a simply constructed one-storey building, located 0.15 km southeast of the station's main building.

1 Meteorological data were collected using automatic meteorological station systems installed

2 at different levels on a tower near the observation building.

3 Although measurements of PAN have been made previously at some high altitude sites in

4 other areas using methods similar to ours (Ford et al., 2002; Fischer et al., 2010; Xue et al.,

5 2011; Pandey Deolal et al., 2013), this is the first report of using the GC-ECD instrument for

6 PAN measurement under the conditions of a high altitude site over 4700 m a.s.l. During the

7 observation period in 2011, the instrument performance was somewhat instable, probably

8 affected by the extreme ambient conditions at the site. The variation of environment

9 temperature is suspected to have made it hard to keep the ECD inner temperature constant.

10 This resulted in abrupt fluctuations in the 10-min chromatographic PAN signals sometimes

11 during the measurement period in 2011. The instable performance of ECD caused varying

12 detection sensitivity. Normally, we convert PAN signals of air samples to concentration data

13 based on ratios of signals to theoretical PAN concentration of the standard gas produced

14 during the calibration. However, the jumping sensitivity makes it improper to obtain PAN

15 concentrations using the normal method. Thus we applied another method, which we call the

16 indirect calibration. Our GC-ECD instrument is optimized for the separation and detection of

17 both PAN and CCl_4. Therefore, it is possible to indirectly calculate the PAN concentration,

18 i.e., by using the ratio of the PAN to CCl4 signal. Details about the indirect calibration are

19 given in the supplement.

20 Although the indirect calibration is a viable way to obtain PAN concentrations, the

21 uncertainty of final data could be larger primarily due to the two assumptions mentioned in

22 the supplement and some technical problems with the observation system. We are more

23 confident of the data from 16 to 25 August 2011. During this period, the instruments

24 performed well and the two calibrations before and after this period gave almost identical

25 sensitivity. In view of this, we report and analyze in this paper mainly data from 16 to 25

26 August 2011, together with those obtained from 15 May to 10 July 2012, where our

27 instruments worked stably.

28 **2.3 Meteorological data and analysis**

29 Local meteorological variables, including temperature, relative humidity, 3-dimensional

30 winds, etc., were observed by corresponding sensors installed at 2 m, 10 m, and 20 m of the

31 meteorological tower at the NMC station. The National Centers for Environmental Prediction

1   (NCEP) reanalysis data, together with the local meteorological data, are used in this paper to

2   facilitate the interpretation of our PAN and O_3 measurements. Global Data Assimilation

3   System (GDAS, 3 hourly, $1°\times1°$ in longitude and latitude, and 26 pressure levels,

4   http://ready.arl.noaa.gov/gdas1.php) was obtained from National Oceanic and Atmospheric

5   Administration (NOAA) Air Resources Laboratory (ARL). The GDAS data were used as

6   input to the Hybrid Single-Particle Lagrangian Integrated Trajectory (HYSPLIT) model (V4.9)

7   for simulating backward air trajectories ending at 500 m and 1500 m above the NMC site.

8   The HYSPLIT model is developed by NOAA/ARL (Draxler and Hess, 1997). In addition,

9   NCEP FNL(final) Operational Global Analysis data (6 hourly, $1°\times1°$ in longitude and

10 latitude, and 26 pressure levels, http://rda.ucar.edu/datasets/ds083.2/#!description) were

11 acquired from National Center for Atmospheric Research (NCAR). These data were used to

12 obtain meteorological fields for analyzing weather patterns and air circulations over the TP.

13 **3   Results and discussion**

14 **3.1   Surface concentrations of PAN and O_3**

15 The PAN concentration averaged 0.36 ppb in the period of 16-25 August 2011, ranging from

16 0.11 ppb to 0.76 ppb. A clear increasing trend is found in the time series of PAN data in this

17 period. The origin of increasing PAN in such period will be discussed in section 3.2. In 2012,

18 the effective observation covered nearly two months (from 15 May to 13 July), long enough

19 to obtain the PAN levels under different atmospheric conditions during the South Asian

20 Monsoon period. The observed PAN concentration in this period varied from 0.16 ppb to 0.99

21 ppb, with an average of 0.44 ppb. This result is close to the PAN levels observed in summer

22 2006 at Waliguan (WLG), a remote site at the northeastern edge of the TP (Xue et al., 2011).

23 The O_3 concentration varied from 27.9 ppb to 96.4 ppb, with an average of 60.0 ppb, nearly

24 identical to the average O_3 level at WLG. There were little day-to-day and diurnal variations

25 when the PAN and O_3 measurements from WLG were not impacted by relatively polluted

26 airmasses from the eastern sector (Xue et al., 2011). In contrast, our PAN and O_3

27 measurements from NMC show profound variations. The reasons of the variations,

28 particularly the diurnal variations, should be investigated.

3.2 Diurnal cycles of PAN and O_3 and potential impacts from the PBL evolution

The 10-min PAN and O_3 concentrations observed in 2012 were used to obtain the averaged diurnal patterns (Fig. 2). As can be seen in Fig. 2, during night time both PAN and O_3 show a decreasing trend and reach the valley around 5:00 Local Time (LT, here LT=Beijing Time – 2h), demonstrating their steady loss during night. From 5:00 LT to 10:00 LT, both gases can be characterized by rapid increase, with the average levels of PAN and O_3 being lifted over 0.10 ppb and 15.0 ppb, respectively. Subsequently, O_3 increases at a much lower rate before reaching its peak around 16:00 LT and then starts to decline. Unlike O_3, PAN behaves more fluctuating after its peak time (around 12:00 LT), with a larger deviation from the trace of O_3.

It is noteworthy to see the sharp early-morning increase of PAN and O_3 shown in Fig. 2. If the observed increase of both gases had been caused by photochemical productions, considerable amount of their precursors would be required to fuel the photochemical reactions. However, according to the EDGAR 3.2FT2000 database, anthropogenic emission in TP is extremely low, with emissions of NO_x and CO being respectively no more than 0.1×10^{-12} kg/m^2/s and 1×10^{-12} kg/m^2/s in the surrounding areas (http://themasites.pbl.nl/tridion/en/themasites/edgar /emission_data/edgar_32ft2000/index-2.html). Surface NO_x at NMC was below the lower detect limit of the commercial NO_x analyzers like TE42CTL and Eco Physics CLD88p that we deployed there. In addition, the key condition for the photochemistry, i.e., the UV radiation, is not expected to be strong enough to drive the photochemistry in the very early morning (say around 5:00 LT), as the sunrise in that TP area occurs around 6:00 LT in summer. Therefore, it is hypothesized that the main factor driving PAN and O_3 ascending in the early morning is not photochemistry but the mixing process during the PBL evolution. To prove this hypothesis, we display scatter plots in Fig. 3, showing the correlations between the increment of O_3 concentration (ΔO_3) and that of PAN concentration (ΔPAN) for two time periods of the day, and the correlation between the increments of O_3 and temperature (ΔT). Figure 3(a) represents data from the 5:00-9:00 LT period, when the solar radiation becomes gradually intensive. Figures 3(b) and 3 (c) show data from the 2:00-4:00 LT period, when no solar radiation is available for the local photochemical reactions.

Significant linear correlation between ΔO_3 and ΔPAN is found for both the early morning period (Fig. 3(a)) and the dark period (Fig. 3(b)), with correlation coefficients of 0.745 and 0.711, respectively. Although photochemical reactions, in which both O_3 and PAN are

1   produced, can lead to the ΔO_3-ΔPAN correlation, they cannot occur during the dark period.

2   Therefore, the significant correlation in Fig. 3(b) should be attributed to some meteorological

3   processes instead of photochemical process. Moreover, the ΔO_3-ΔT correlation shown in Fig.

4   3(c) further indicates that surface O_3 and PAN at the site may be changed purely due to some

5   meteorological processes that change air temperature as well. The net change of O_3 could be

6   positive before dawn, and occurred on those days with simultaneously rising PAN and

7   temperature. The rising temperature could be related to the dry adiabatic heating process

8   during air masses sinking. Such a process happens when the PBL is extended, not necessarily

9   driven by solar radiation. Downward transport of PAN and O_3 may accompany such process.

10   Therefore, the PBL evolution might have significantly impacted the diurnal variations of PAN

11   and O_3 at NMC.

12   ### 3.3   Insight into the PBL evolution

13   The evolution of PBL plays one of the key roles in the diurnal variations of surface

14   meteorological parameters and air pollutants, and is influenced by the dominating synoptic

15   situation. It has different diurnal patterns under different synoptic situations. Here we take the

16   O_3 enhancement in the early morning as an indicator quantity to find out major differences in

17   the evolution of the PBL and some related parameters under different synoptic situations. We

18   selected 30 days from the observation period in 2012 and separated them into two groups,

19   with group one including 15 days with the greatest ΔO_3 values (High ΔO_3) and group two

20   including 15 days with the smallest ΔO_3 values (Low ΔO_3). For the two groups, average

21   diurnal variations were calculated of PAN, O_3 and some meteorological parameters, i.e., wind

22   speed at 2 m above ground (Ws), U wind speed at 2 m above ground (Us), V wind speed at 2

23   m (Vs), the ratio between the 2-m and 10-m wind speeds (WSR), the temperature difference

24   between 20 m and 10 m (TD), and water vapor pressure (WVP). The obtained diurnal

25   variations are plotted in Fig. 4.

26   A stable nocturnal boundary layer (NBL) forms gradually in the night (Stull, 1988). A

27   temperature inversion occurs in the NBL, with the air temperature increasing with height. A

28   nocturnal jet may form over the NBL so that a larger gradient of wind speed exists in the NBL.

29   Such stratification prevents the air from being vertical mixed in the night and is broken in the

30   early morning. As a result, the concentrations of O_3 and PAN at the ground-level decrease

31   largely in the nighttime because of chemical and physical losses and increase rapidly in the

32   early morning because of the downward mixing of upper-level air containing more O_3 and

1 PAN. This evolution of PBL, however, can be strongly impacted by some systematic

2 processes so that the day-night differences of PBL are weakened or even disappear. We

3 believe that the two groups of data presented in Fig. 4 represent approximately two

4 circumstances of the PBL evolution, with the High-ΔO_3 group being less or not impacted and

5 the Low-ΔO_3 group being strongly impacted by the systematic processes.

6 As can be seen in Fig. 4, the Low-ΔO_3 group showed much smaller diurnal variations of PAN,

7 O_3, Ws, WVP, and WSR, suggesting a weak day-night cycle of the PBL. Compared with the

8 values in the Low-ΔO_3 group, the nighttime values of PAN, O_3, Ws, and WSR in the High-

9 ΔO_3 group were much lower, and that of TD much higher. Lower WSR and higher TD in the

10 night indicate a more stable NBL, which explains the lower PAN and O_3 levels as discussed

11 above. After dawn the values of PAN, O_3, Ws, WSR, and TD in the High-ΔO_3 group changed

12 rapidly back to their daytime levels, indicating the break of the stable NBL. It is noteworthy

13 that there were virtually no or only minor differences in the daytime values of PAN, Ws,

14 WSR, and TD between the two groups. The daytime O_3 in the High-ΔO_3 group reached

15 significantly higher levels than that in the Low-ΔO_3 group. Moreover, the WVP value in the

16 High-ΔO_3 group was lower than that in the Low-ΔO_3 group during the entire day. These

17 phenomena imply that the High-ΔO_3 group is related to drier days and PBL conditions

18 favoring the increase of surface O_3 during daytime (e.g., through downward mixing) and

19 destruction during nighttime, while the Low-ΔO_3 group is related to more humid days and

20 PBL conditions that inhibit the variation of surface O_3.

21 The PBL evolution was investigated in previous field experiments in the TP. Li et al. (2011)

22 found that there were some differences in the diurnal evolution of the PBL structure between

23 dry and rainy seasons. In the dry season, namely the pre-monsoon period, a shallow but strong

24 inversion layer could be clearly observed at night. The occurrence of the inversion layer is

25 high in the pre-monsoon period, simply because the PBL structure is primarily driven by

26 sensible heat (Ma et al., 2005). The outflow of sensible heat at night is massive according to

27 thermal analysis. In the rainy season, a shallower but more persistent wet convection evolves,

28 forcing efficient exchange of quantities and also comparably smaller gradients of

29 meteorological elements. The daytime PBL height can reach 4-5 km above the ground in the

30 dry pre-monsoon period, while it is usually about 1-2 km above the ground in the wet

31 monsoon period (Li et al., 2011; Chen et al., 2013). In our case, prevailing monsoonal

32 features are perceivable in meteorological measurements associated with the Low-ΔO_3 group,

1   such as the stronger southerly wind (Fig. 4(h)) and higher WVP (Fig. 4(d)). Unlike the dry

2   season, the convection intensity in the wet season has a much smaller diurnal variation, as

3   suggested by the smaller day-night differences of WSR and TD. Thus in the wet season,

4   downward transport of PAN and O_3 during nighttime may be much more effective than that in

5   the dry season. This can explain the observed nighttime differences in the PAN and O_3

6   concentrations between the Low-ΔO_3 and High-ΔO_3 groups (Figs. 4(a) and 4(b)).

7   To know more details about the two groups of days discussed above, the distribution of the

8   two groups of days, together with parameters including the PBL height, precipitable water of

9   entire atmosphere (PWAT), WVP, and the PAN and O_3 concentrations are shown in Fig. 5.

10   The PBL height and PWAT values are obtained from the NCEP FNL reanalysis data. It can

11   be seen that the surface measured WVP is in good accordance with the PWAT in trend. The

12   whole observation period in 2012 can be divided into dry period and wet period. The

13   transition between the wet and dry periods can be easily identified based on the changes of the

14   PBL height, and the PWAT and WVP values. It can also be seen in the variation of the daily

15   rainfall at NMC (Fig. S1). We can see a sudden seasonal change in the middle of June, when

16   the depth of PBL was suppressed after 16 June 2012 (marked with green bar in Fig. 5) and the

17   water amount became more abundant, suggesting the onset of the South Asian monsoon. The

18   distributions of the two groups of days are labeled on Fig. 5(a). Although there are some

19   irregular cases, the High-ΔO_3 days (group 1) are mostly distributed in the dry period and the

20   Low-ΔO_3 days (group 2) in the wet period. This supports our analysis in previous paragraph.

21   The time series of the PBL height indicates that the daily maximum PBL heights in the dry

22   period were much higher than those in the wet period, with only a few exceptions. Such

23   phenomenon agrees with the observational results from Naqu, about 230 km northeast of

24   NMC (Li et al., 2011). The nocturnal PBL height in the dry period could be extremely low

25   (frequently lower than 200 m). This explains the lower nighttime PAN and O_3 values in the

26   High-ΔO_3 group (Fig. 4).

27   In the pre-monsoon there may be episodes with monsoon features. An example of this is the

28   period of a few days around early June 2012, where the PBL height was considerably

29   suppressed, and the PWAT, WVP as well as the concentrations of PAN and O_3 were

30   significantly enhanced (Fig. 5). In this relatively humid episode, the nighttime concentrations

31   of PAN and O_3 were largely elevated, which may be attributable to the PBL structure and

32   airmasses transported from the polluted region (see section 3.5).

1   In conclusion, the South Asian monsoon brings not only more water vapor over the central

2   Tibet area but also effectively drives the PBL evolution, which plays an important role in

3   shaping the diurnal patterns of PAN and O_3 at the NMC site.

4   **3.4 PAN abundance in upper levels**

5   It is noticeable in Fig. 4 that the levels of daytime O_3 were considerably different between the

6   two groups, while those of daytime PAN were close to each other. The highest hourly O_3

7   concentrations for the two groups were 69.7 ± 2.4 ppb and 59.0 ± 2.5 ppb, respectively, and the

8   highest hourly PAN concentrations were 0.48 ± 0.02 ppb and 0.49 ± 0.05 ppb, respectively. Xue

9   et al. (2011) pointed out that air masses from higher altitudes (upper troposphere/lower

10   stratosphere) could have significant impact on surface O_3 in the plateau. As shown in Fig. 5,

11   the daytime PBL heights in group 1 could extend to much higher altitudes than those in group

12   2, indicating a higher probability of downward mixing of O_3–richer air from the middle and

13   upper troposphere on the days in group 1. The air masses from higher altitudes seemed not to

14   cause additional increase in the daytime level of surface PAN, as suggested by the negligible

15   distinction of daytime PAN between groups 1 and 2.

16   To gain more insight in air masses from upper origins, we attempt to label the upper air

17   masses in the whole observation periods. Following the categorizing way in section 3.3,

18   scatter plots of PAN- O_3, WVP- O_3, and WVP-PAN are shown in Fig. 6 for the two groups.

19   Since we have confirmed the meteorological features associated with both groups, some

20   relationship characteristics could be well comprehended. Suppose photochemistry did not

21   vary considerably, the amount of O_3 could in some degree represent the impact of upper

22   airmass. Using the Tropospheric Emission Spectrometer (TES) observations, Worden et al.

23   (2009) elaborately depicted the 3-dimensional distribution of tropospheric O_3 over the TP and

24   its surrounding areas, which shows a gradual increase of the O_3 concentration with height

25   under tropopause and a steep increase from upper troposphere to lower stratosphere. In some

26   cases, air masses with O_3 higher than 100 ppb can be downward transported to near ground,

27   causing high surface O_3 events. Thus surface O_3 concentration in the TP region can be used as

28   an indicator of air masses from the higher altitudes and also reflects the depth of developed

29   PBL. As the WVP profile shows a clear decrease with height (Chen et al., 2013), air masses

30   from high altitudes can also be indicated by lower WVP. The data points within the red

31   rectangle in Fig. 6(c) are measurements associated with higher O_3 levels and lower WVP. We

32   consider these as measurements with significant features of middle/upper tropospheric air.

1   Fig. 6(b) displays a good positive PAN-O_3 correlation for group 2, which is consistent with

2   simultaneous photochemical production of both secondary oxidants. However, the dataset

3   from group 1 shows a much weaker PAN-O_3 correlation (Fig. 6(a)), indicating a more obscure

4   relationship between PAN and altitude in group 1. Nearly no correlation between PAN and

5   WVP is found (Fig. 6(e)), supporting the above viewpoint. At present, the actual causes of the

6   poor PAN-O_3 and PAN-WVP correlations are unknown. However, it is reasonable to believe

7   that on the days in group 1, the observed O_3 level was more influenced by air masses from

8   upper troposphere/lower stratosphere, where the O_3 level is high (Worden et al., 2009) but the

9   PAN level is low (Moore and Remedios, 2010). In addition, it is suspected that the horizontal

10   variability of PAN is larger than that of O_3.

11   The ambiguity in the relationship between PAN and altitude makes it impossible to estimate

12   the PAN abundance in upper levels simply from the data shown in Fig. 6. Nevertheless, we

13   can make use of some cases with deep convection and apparent downward transport activities

14   in the dry period. Here we try to deduce the origins of air masses in two cases and roughly

15   estimate the PAN concentrations in upper levels. The two cases chosen for analysis are 25

16   May 2012 and 24 August 2011. Figure 7 displays the omega field and horizontal wind vectors

17   at different time and pressure height, with the two cases labeled by red rectangles (termed as

18   Case 1 and Case 2). Both cases are segments of the dry periods, when the PBL could reach

19   higher heights and favor the entrainment of upper air-masses.

20   Figure 7(a) shows that positive omega dominated the PBL from early 25 May 2012 to early

21   26 May 2012 (Case 1), with the range of higher omega (>0.1 m/s) extending from surface to

22   350 hPa, and a distinct valley of specific humidity line of 2g/kg, indicating a strong

23   downward motion core. In response to this downward transport, PAN and O_3 were both

24   elevated to higher levels and WVP dropped (Fig. 5). A similar downward motion core

25   occurred on 22-23 August 2011 (Case 2), as shown in Fig. 7(b). The downdraft motion core

26   on 22 August extended up to 300 hPa and lasted all day long, with very high intensity

27   (omega > 0.4 m/s) after the noontime. For better understanding of Case 2, we display the time

28   series of O_3, PAN, and related meteorological parameters in Fig. 8. There was a rapid rising

29   trend of the O_3 and PAN levels on 22 August 2011, as indicated by the arrow in Fig. 8(b). In

30   parallel with this trend, relative humidity and wind vector changed sharply, with the former

31   dropping dramatically from 80% to about 30% and the later turning from southerly to

1   northerly. Similar rapid variations were also observed partly during 23-24 August 2011,

2   corresponding to the subsiding of dry air masses (Fig. 7(b)).

3   It is noticeable that the daytime levels of O_3 and PAN did not show much distinction among

4   the days from 22 to 25 August 2011. This suggests that the air masses measured during the

5   period might originate from the similar height and area. To prove this, we calculated

6   backward trajectories with endpoints at 500 m and 1500 m above the ground of the NMC site.

7   Some of the trajectories for the two selected cases, 25 May 2012 (Case 1) and 22 August 2011

8   (Case 2), are plotted in Figs. 9 and 10, respectively, overlaying on the 250 hPa potential

9   vorticity (PV) fields at three timepoints during 23-24 May 2012 (for Case 1) and during 20-22

10 August 2011 (for Case 2), respectively. Similar plots with the same trajectories and 350 hPa

11 PV fields are shown in Figs. S2 and S3 for Case 1 and Case 2, respectively. In both cases

12 stratospheric intrusions occurred as indicated by the higher PV values. In Case 1 (Figs. 9 and

13 S2) higher PV covered the zone from 30 °N to beyond 50 °N. In Case 2 (Figs. 10 and S3)

14 higher PV extended from about 40 °N to beyond 50 °N. In both case air masses arrived at the

15 NMC site originated from or travelled through the zones obviously impacted by stratospheric

16 intrusions. Therefore, the PAN and O_3 measurements in both cases were influenced by upper

17 level air masses that cantained stratospheric air. In addition to this transport feature, the

18 rapidly increasing O_3 and decreasing water amount also indicate that surface air masses

19 originated from high levels. For Case 1 and Case 2, the PAN concentration was elevated

20 respectively up to 0.5 ppb and 0.6-0.7 ppb, which can be regarded as the estimated level of

21 PAN at high altitudes (around 350 hPa).

22 Table 1 summarizes the PAN levels in the upper troposphere over the TP. A prominent

23 progress in detection of global upper-tropospheric PAN is based on the application of infra-

24 red spectrometers. There exists some detection error as retrieval band of PAN would

25 inevitably be contaminated by irrelevant compounds, such as water vapor and CCl_4 and the

26 variability of some atmospheric parameters would also bring interferences (Remedios et al.,

27 2007). In summer, there exists more uncertainty using remote sensing method due to higher

28 amount of water vapor over the TP region; hence a direct comparison with field measurement

29 is required. According to the satellite results (Moore and Remedios, 2010), the retrieved PAN

30 levels at 333 hPa and 234 hPa in March 2003 were in the ranges of 0.3-0.5 ppb and 0.15-0.2

31 ppb, respectively, implying a decreasing trend of the PAN concentration along height in the

32 upper troposphere. In August 2003 the PAN levels at 278 hPa and 185 hPa did not show

1 evident increment compared with March 2003. Model results from Fischer et al. (2014) show

2 similar ranges of PAN levels. The trajectories shown in Figs. 9, 10, S2 and S3 indicate that air

3 masses could originate from the upper troposphere (~350 hPa), thus could well match the

4 other observation heights listed in Table 1. Our estimates of PAN level are close to or greater

5 than the upper ranges of the PAN levels reported in the literature (Glatthor et al., 2007; Moore

6 and Remedios, 2010; Wiegele et al., 2012; Fadnavis et al., (2014; Fischer et al., 2014). Taking

7 into account the thermal decomposition and photolysis of PAN during the transport, the actual

8 PAN levels in the upper troposphere could be higher than our estimates. Therefore, the

9 retrieval from MIPAS-E measurements might have underestimated the PAN level in the upper

10 troposphere.

11 Moreover, an enhancement of PAN was observed during 21-26 August 2011, with a range of

12 0.6-0.7 ppb, indicating that PAN was accumulated in an elevated level in later summer. Such

13 PAN level was not acquired by Moore and Remedios (2010) who reported a maximum of

14 PAN of 0.5 ppb in August, implying again the possibility of underestimation of PAN in

15 satellite retrieval. It is noted that the satellite observations were made years before our

16 measurements. Any potential long-term changes or interannual variations in PAN may also

17 cause some differences. Fadnavis et al. (2014) reported a maximum increase rate of 4.5±3.1

18 ppt yr^{-1} for PAN in the UTLS over the Asian summer monsoon region in the summer

19 monsoon season during 2002-2011. However, such small trend in PAN cannot explain the

20 above discrepancy.

21 **3.5   A PAN episode driven by South Asian monsoon**

22 In warm environment, PAN is short-lived. Below 7 km, thermal decomposition is the main

23 loss process of PAN (Talukdar, 1995). Thus although polluted air masses from south of the

24 Himalayas can be transported to TP along the monsoon stream, PAN in the air masses may

25 experience great loss during the travelling. The level of PAN observed at our site was the

26 remaining PAN in the air masses, which should be significantly lower than that in the

27 formation area. Nevertheless, PAN episodes can be observed under certain meteorological

28 conditions. One of such episodes occurred in early June 2012. As can be seen in Fig. 5, the

29 PAN level humped during 1-6 June 2012, with some diurnal variations. The maximum PAN

30 level reached 1.0 ppb, and the diurnal minima on these days were even higher than the diurnal

31 maxima on many of other observation days. The origin of the high PAN concentrations

32 deserves investigation.

1   Data in Fig. 5 indicate that the monsoon flow prevailed persistently after the middle of June

2   2012, and there were also some features of monsoon impact during 1-6 June 2012 when the

3   PAN level was increased to near 1 ppb. After this abrupt rising, PAN dropped down to much

4   lower level, suggesting a substantial change in air mass. To understand this phenomenon, we

5   calculated average fields of wind, relative humidity, and omega at sigma=0.995 for the

6   periods 30-31 May using the FNL reanalysis data. During 30-31 May 2012, the major part of

7   Indian subcontinent was controlled by an anticyclone system and a large convergence zone

8   formed over the central TP (see Fig. S4). The NMC site was within this convergence zone and

9   obviously influenced by airflow from North India. Figure 10 shows the average wind fields

10   for 12:00 (UTC) of 4, 5, 7 and 8 June 2012. These wind fields can help us to understand the

11   high level of PAN observed during 1-6 June 2012. As can be seen in Figs. 11 and S4, the

12   week after 30 May the NMC site was under the control of a large convergence zone and

13   influenced by westerly and southwesterly winds, which could transport air masses from North

14   India to the NMC site. After this period, the site was influenced by significantly different air

15   masses. For example, the average wind field shown in Figs. 11c and 11d indicate that after 7

16   June 2012, strong southerly and southeasterly winds developed over East India and Southeast

17   Nepal, and the area surrounding NMC was controlled by southerly wind, which promotes the

18   transport of air masses from the Bay of Bengal. Although most of the central and western TP

19   was still under the control of the convergence zone, NMC and its surrounding were outside of

20   its direct impact. Such change in air masses arriving NMC inevitably caused substantial

21   differences in photochemistry. As indicated by observations (Ghude et al., 2008; Fishman et

22   al., 2003), Northern India suffers photochemical pollution. Emission inventories (Ohara et al.,

23   2007; Zhang et al., 2009) suggest that North India is one of the Asian emission centers for

24   pollutants including NO_x and VOCs. Tropospheric NO_2 and HCHO can be derived from

25   satellite observations based on the DOAS technique (Boersma et al., 2011; De Smedt et al.,

26   2008, 2012). Figure S5 shows tropospheric NO_2 and HCHO columns during June, 2012,

27   made available by the Tropospheric Emission Monitoring Internet Service (TEMIS) at The

28   Royal   Netherlands   Meteorological   Institute   (KNMI),   The   Netherlands

29   (http://www.temis.nl/index.php). As can be seen in this figure, both NO_2 and HCHO in the

30   troposphere over North India were highly abundant in June, 2012. The high NO_2 and HCHO

31   concentrations suggest that the concentrations of NO_x and VOCs over the North India region

32   were high. NO_x and VOCs are species for photochemical reactions leading to formation of O_3,

1 PAN, etc. Therefore, it is likely that the PAN episode observed at our site during 1-6 June

2 2012 was mainly caused by plumes with high PAN and its precursors from North India.

3 To further support the above view, we made calculations of backward air trajectories. The

4 results are presented in Fig. 12. The 5-day trajectories were calculated for endpoints at 500 m

5 and 1000 m above ground for 1-6 June and 7-10 June 2012, respectively. Obviously, air

6 trajectories arriving NMC during 1-6 June were quite different from those during 7-10 June,

7 particularly those with endpoints at 500 m (Figs. 12a and 12c). About a half of the trajectories

8 during 1-6 June originated from or moved through the PBL over North India (Fig. 12a), while

9 nearly none of the trajectories during 7-10 June had an opportunity to pass through the PBL

10 over North India (Fig. 12c). Most of the trajectories during 7-10 June originated either from

11 the free troposphere over western Asia and Indian subcontinent or from the PBL south of

12 NMC. These can explain the sudden decrease of the PAN level after 6 June 2012 on one hand,

13 and on the other hand support the idea that the PAN episode observed during 1-6 June 2012

14 was mainly caused by plumes from North India.

15 Although the TP is one the cleanest regions of the world, transport of anthropogenic

16 pollutants deserves attention. Some recent studies have showed that air pollutants can be

17 transported to the Himalayas or to the TP region through passes like river valleys from the

18 surroundings (Cong et al., 2007; Cong et al., 2009; Bonasoni et al., 2010; Kopacz et al., 2011;

19 Lüthi et al., 2015; Shen et al., 2015; Zhang et al., 2015). The main source regions are South

20 and East Asia. During the South Asian monsoon, the TP is predominately influenced by air

21 masses from the Indian subcontinent. Impacts of transported pollutants on atmospheric

22 environment over the Himalayas and TP, particularly the climate and hydrological effects of

23 deposition of black carbon and other substances on Himalayan glaciers, have caused concerns

24 (Ramanathan et al., 2007; Ming et al., 2012; Zhao et al., 2013; Qu et al., 2014; Wang et al.,

25 2015; Zhang et al., 2015).

26 So far, studies of transport of pollutants to the TP and its effect are mainly about aerosols

27 (compositions and optical depth) and less attention has been paid to gaseous pollutants. There

28 has been no previous report about impacts of long-range transport of pollutants on

29 tropospheric photochemistry over the TP region. Our results show, for the first time, that

30 long-range transport of polluted airmasses from North India can significantly enhance

31 ambient level of PAN at NMC. Although we have no observational data of PAN from other

32 sites in the TP, it is likely that the entire convergence zone in the central and western TP (Figs.

1 10 and S4) was more or less impacted by the pollutants from North India. This implies that

2 photochemistry over a large area in the TP was probably disturbed for at least ten days in the

3 cases shown in Figs. 11 and S4. PAN transported to the TP region may be thermally and/or

4 photolytically decomposed to release NO_x, acting as a chemical source of atmospheric NO_x

5 over the TP, a region with very little anthropogenic emission of NO_x. The impacts of the

6 transport of PAN and other related species on tropospheric photochemistry over the TP need

7 to be studied in the future.

8 **4 Conclusions**

9 For the first time, we made simultaneous ground-based measurements of two photochemical

10 products, PAN and O_3 at Nam Co, a remote site in the central Tibetan Plateau (TP) region.

11 Our effective PAN data cover two summer periods, i.e., 16-25 August 2011 and 15 May to 13

12 July 2012. The average concentrations of PAN were 0.36 ppb (range: 0.11-0.76 ppb) and 0.44

13 ppb (range: 0.21-0.99 ppb) in the 2011 and 2012 periods, respectively. During the observation

14 in 2012, the O_3 concentration varied from 27.9 ppb to 96.4 ppb, with an average of 60.0 ppb,

15 very close to the summertime O_3 level found at Waliguan, a global baseline station at the

16 northeastern edge of the TP.

17 PAN and O_3 showed profound and similar diurnal cycles, with valleys around 5:00 LT, steep

18 rises in the early morning, and broader platforms of high values during 9:00-20:00 LT. Such

19 patterns of diurnal variations of both gases, particularly the sharp increases even before

20 sunrise, cannot be attributed solely to local photochemistry. Our analysis suggests that the

21 PBL evolution played a key role in shaping the diurnal patterns of both oxidants. PAN and O_3

22 in the shallow nocturnal PBL were significantly removed by their sinks, such as chemical

23 reactions and dry deposition. In the early morning, the elevation of the PBL height caused

24 downward mixing of upper air containing higher PAN and O_3, leading to steep rises of the

25 concentrations of these gases. The downward mixing and photochemistry sustained the higher

26 levels of PAN and O_3 in the daytime. However, there were day-to-day differences in the PBL

27 evolution, which could cause large differences in the diurnal variations of PAN and O_3. We

28 identified two groups of days with different meteorological conditions and different diurnal

29 patterns of trace gases and meteorological parameters. Days in group 1 were mainly

30 distributed in the pre-monsoon period, with higher daytime height of PBL (about 3 km), lower

31 humidity, and larger day-night variations of PAN and O_3. Days in group 2 were mainly

1 distributed in the monsoon period, with shallower daytime PBL (about 2 km), higher

2 humidity, and much smaller day-night variations of PAN and O_3.

3 There were some cases with obvious rapid transport of air masses during our observations.

4 We identified two cases of rapid downward transport of air masses from the middle and upper

5 troposphere. The observed PAN levels during these two cases ranged from 0.5 ppb to 0.7 ppb.

6 They may represent those in the middle and upper troposphere. These PAN levels are higher

7 than those retrieved from satellite measurements. In addition to vertical transport of PAN, we

8 also identified a case of strong long-range transport of PAN plumes. During this case,

9 relatively polluted air masses from the PBL over North India were able to be transported over

10 the western and central TP to NMC, causing a profound episode of PAN with maximum close

11 to 1 ppb during 1-6 June 2012. In contrast, significantly lower PAN levels were observed

12 when air masses originated from other areas. Although transport of aerosols from South and

13 Southeast Asia and its impacts on atmospheric environment over Himalayas and the TP have

14 been intensively studied in recent years, gaseous pollutants have received less attention. Our

15 results show, for the first time, that polluted air masses from South Asia can significantly

16 enhance the ambient level of PAN at NMC. The space scale and frequency of this

17 phenomenon and its impacts on tropospheric photochemistry over the TP region remain to be

18 studied in the future.

19 **Data availability.** The observational data analyzed in this paper can be made available for

20 scientific purposes by contacting the corresponding author (xuxb@camscma.cn).

21 **Competing interests.** The authors declare that they have no conflict of interest.

22 **Acknowledgements.** The authors thank the staff of the Nam Co station and Xizang

23 Meteorological Bureau for logistical support. This work was supported by the China Special

24 Fund for Meteorological Research in the Public Interest (GYHY201106023), the Natural

25 Science Foundation of China (No.41330422) and Basic Research Fund of CAMS (2011Z003

26 and 2013Z005).

1 References

2 Bonasoni, P., Laj, P., Marinoni, A., Sprenger, M., Angelini, F., Arduini, J., Bonafè, U.,
3 Calzolari, F., Colombo, T., Decesari, S., Di Biagio, C., di Sarra, A. G., Evangelisti, F., Duchi,
4 R., Facchini, M. C., Fuzzi, S., Gobbi, G. P., Maione, M., Panday, A., Roccato, F., Sellegri, K.,
5 Venzac, H., Verza, G. P., Villani, P., Vuillermoz, E., and Cristofanelli, P.: Atmospheric
6 Brown Clouds in the Himalayas: first two years of continuous observations at the Nepal
7 Climate Observatory-Pyramid (5079 m), Atmos. Chem. Phys., 10, 7515-7531, 2010.

8 Boersma, K.F., Eskes, H.J., Dirksen, R. J., van der A, R. J., Veefkind, J. P., Stammes, P.,
9 Huijnen, V., Kleipool, Q. L., Sneep, M., Claas, J., Leitao, J., Richter, A., Zhou, Y., and
10 Brunner, D.: An improved retrieval of tropospheric NO_2 columns from the Ozone Monitoring
11 Instrument, Atmos. Meas. Tech. , 4, 1905-1928, 2011

12 Chen, B., Xu, X. D., Yang, S., and Zhao, T. L.: Climatological perspectives of air transport
13 from atmospheric boundary layer to tropopause layer over Asian monsoon regions during
14 boreal summer inferred from Lagrangian approach, Atmos. Chem. Phys., 12, 5827-5839,
15 10.5194/acp-12-5827-2012, 2012.

16 Chen, X., An, J. A., Su, Z., Torre, L., Kelder, H., Peet, J., Ma, Y., and Fu, R.: The Deep
17 Atmospheric Boundary Layer and Its Significance to the Stratosphere and Troposphere
18 Exchange over the Tibetan Plateau, PloS One, 8, e56909, 10.1371/journal.pone.005690, 2013.

19 Cong, Z. Y., Kang, S. C., Liu, X. D., and Wang, G. F.: Elemental composition of aerosol in
20 the Nam Co region, Tibetan Plateau, during summer monsoon season, Atmos. Environ., 41,
21 1180–1187, 2007.

22 Cong, Z. Y., Kang, S., Smirnov, A., and Holben, B.: Aerosol optical properties at Nam Co, a
23 remote site in central Tibetan Plateau, Atmos. Res., 92, 42–48, 2009.

24 Cox, R.A. and Roffey, M.J.: Thermal decomposition of peroxyacetylnitrate in the presence of
25 nitric oxide. Environ. Sci. & Technol., 11(9), 900–906,1977.

26 Cristofanelli, P., Bracci, A., Sprenger, M., Marinoni, A., Bonafè, U., Calzolari, F., Duchi, R.,
27 Laj, P., Pichon, J. M., Roccato, F., Venzac, H., Vuillermoz, E., and Bonasoni, P.:
28 Tropospheric ozone variations at the Nepal Climate Observatory-Pyramid (Himalayas, 5079m
29 a.s.l.) and influence of deep stratospheric intrusion events, Atmos. Chem. Phys., 10, 6537–
30 6549, 2010.

1   De Smedt, I., Van Roozendael, M., Stavrakou, T., M üller, J.-F., Lerot, C. , Theys, N., Valks,

2   P., Hao, N., and van der, N.A.: Improved retrieval of global tropospheric formaldehyde

3   columns from GOME-2/MetOp-A addressing noise reduction and instrumental degradation

4   issues. Atmos. Meas. Tech., 5, 2933-2949, 2012.

5   De Smedt, I., M üller, J.-F., Stavrakou, T., van der, A., R. J., Eskes, H. J., and Van Roozendael,

6   M.: Twelve years of global observations of formaldehyde in the troposphere using GOME

7   and SCIAMACHY sensors, Atmos. Chem. Phys., 8(16), 4947-4963, 2008.

8   Dessler, A. E., and Sherwood, S. C.: Effect of convection on the summertime extratropical

9   lower stratosphere, J. Geophys. Res., 109, D23301-D23310, 10.1029/2004jd005209, 2004.

10   Ding, A. and Wang, T.: Influence of stratosphere-to-troposphere exchange on the seasonal

11   cycle of surface ozone at Mount Waliguan in western China, Geophys. Res. Lett., 33, L03803,

12   doi:10.1029/2005GL024760, 2006.

13   Draxler, R.R. and Hess, G.D.: Description of the HYSPLIT 4 modeling system. NOAA

14   Technical Memorandum. ERLARL–224, NOAA Air Resources Laboratory, Silver Spring,

15   MD. 24, 1997.

16   Fadnavis, S., Schultz, M.G., Semeniuk, K., Mahajan, A.S., Pozzoli, L., Sonbawne, S., Ghude,

17   S.D., Kiefer, M., and Eckert, E.: Trends in peroxyacetyl nitrate (PAN) in the upper

18   troposphere and lower stratosphere over southern Asia during the summer monsoon season:

19   regional impacts, Atmos. Chem. Phys., 14, 12725–12743, 2014.

20   Fischer, E. V., Jaffe, D. A., Reidmiller, D. R., and Jaegle, L.: Meteorological controls on

21   observed peroxyacetyl nitrate at Mount Bachelor during the spring of 2008, J. Geophys. Res.,

22   115, D03302, doi:10.1029/2009jd012776, 2010.

23   Fischer, E. V., Jaffe, D. A., and Weatherhead, E. C.: Free tropospheric peroxyacetyl nitrate

24   (PAN) and ozone at Mount Bachelor: potential causes of variability and timescale for trend

25   detection, Atmos. Chem. Phys., 11, 5641-5654, 10.5194/acp-11-5641-2011, 2011.

26   Fischer, E. V., Jacob, D. J., Yantosca, R. M., Sulprizio, M. P., Millet, D. B., Mao, J., Paulot,

27   F., Singh, H. B., Roiger, A. E., Ries, L., Talbot, R. W., Dzepina, K., and Pandey Deolal, S.:

28   Atmospheric peroxyacetyl nitrate (PAN): a global budget and source attribution, Atmos.

29   Chem. Phys., 14, 2679-2698, 2014.

1   Fishman, J., Wozniak,A.E., and Creilson, J.K.: Global distribution of tropospheric ozone from
2   satellite measurements using the empirically corrected tropospheric ozone residual technique:
3   Identification of the regional aspects of air pollution, Atmos. Chem. Phys., 3, 893–907, 2003.

4   Ford, K. M., Campbell, B. M., Shepson, P. B., Bertman, S. B., Honrath, R. E., Peterson, M.,
5   and Dibb, J. E.: Studies of Peroxyacetyl nitrate (PAN) and its interaction with the snowpack
6   at Summit, Greenland, J. Geophys. Res., 107, 4102-4111, 2002.

7   Fu, R., Hu, Y., Wright, J. S., Jiang, J. H., Dickinson, R. E., Chen, M., Filipiak, M., Read, W.
8   G., Waters, J. W., Wu, D. L., and Affiliations, A.: Short circuit of water vapor and polluted
9   air to the global stratosphere by convective transport over the Tibetan Plateau, PNAS, 103,
10 5664-5669, 10.1073/pnas.0601584103, 2006.

11 Gettelman, A., and Kinnison, D. E.: Impact of monsoon circulations on the upper troposphere
12 and lower stratosphere, J. Geophys. Res., 109, D22101-D22114, 10.1029/2004jd004878,
13 2004.

14 Ghude, S.D., Jain, S.L., Arya, B.C., Beig, G., Ahammed, Y.N., Kumar, A., Tyagi, B.: Ozone
15 in ambient air at a tropical megacity, Delhi: characteristics, trends and cumulative ozone
16 exposure indices, J. Atmos. Chem., 60, 237–252, 2008.

17 Glatthor, N., von Clarmann, T., Fischer, H., Funke, B., Grabowski, U., Hopfner, M.,
18 Kellmann, S., Kiefer, M., Linden, A., Milz, M., Steck, T., and Stiller, G. P.: Global
19 peroxyacetyl nitrate (PAN) retrieval in the upper troposphere from limb emission spectra of
20 the Michelson Interferometer for Passive Atmospheric Sounding (MIPAS), Atmos. Chem.
21 Phys., 7, 2775–2787, doi:10.5194/acp-7-2775-2007, 2007.

22 Gu, Y., Liao, H., and Bian, J.: Summertime nitrate aerosol in the upper troposphere and lower
23 stratosphere over the Tibetan Plateau and the South Asian summer monsoon region, Atmos.
24 Chem. Phys., 16, 6641-6663, doi:10.5194/acp-16-6641-2016, 2016.

25 Hudman, R.C., Jacob, D.J., Cooper, O.R., Evans, M.J., Heald, C.L., Park, R.J., Fehsenfeld, F.,
26 Flocke, F., Holloway, J., Hübler, G., Kita, K., Koike, M., Kondo, Y., Neuman, A., Nowak, J.,
27 Oltmans, S., Parrish, D., Roberts, J.M., and Ryerson, T.: Ozone production in transpacific
28 Asian pollution plumes and implications for ozone air quality in California, J. Geophys. Res.,
29 109, D23S10-D23S23, 10.1029/2004jd004974, 2004.

1 Kopacz, M., Mauzerall, D. L., Wang, J., Leibensperger, E. M., Henze, D. K., and Singh, K.:

2 Origin and radiative forcing of black carbon transported to the Himalayas and Tibetan Plateau,

3 Atmos. Chem. Phys., 11, 2837-2852, 10.5194/acp-11-2837-2011, 2011.

4 LaFranchi, B. W., Wolfe, G. M., Thornton, J. A., Harrold, S. A., Browne, E. C., Min, K. E.,

5 Wooldridge, P. J., Gilman, J. B., Kuster, W. C., Goldan, P. D., de Gouw, J. A., McKay, M.,

6 Goldstein, A. H., Ren, X., Mao, J., and Cohen, R. C.,Closing the peroxy acetyl nitrate budget:

7 observations of acyl peroxy nitrates (PAN, PPN, and MPAN) during BEARPEX 2007, Atmos.

8 Chem. Phys., 9(19), 7623–7641, 2009.

9 Law, K. S.,Fierli, F., Cairo, F., Schlager, H., Borrmann, S., Streibel, M., Real, E., Kunkel, D.,

10 Schiller, C., Ravegnani, F., Ulanovsky, A., D'Amato, F., Viciani, S., Volk, C.M.: Air mass

11 origins influencing TTL chemical composition over West Africa during 2006 summer

12 monsoon, Atmos. Chem. Phys., 10, 10753–10770, 2010.

13 Lelieveld, J., Brühl, C., Jöckel, P., Steil, B., Crutzen, P. J., Fischer, H., Giorgetta, M. A., Hoor,

14 P., Lawrence, M. G., Sausen, R., and Tost, H.: Stratospheric dryness: model simulations and

15 satellite observations, Atmos. Chem. Phys., 7, 1313-1332, 2007.

16 Lelieveld, J. and Dentener, F. J.: What controls tropospheric ozone? J. Geophys. Res.,

17 105(D3), 3531–3551, 2000.

18 Li, M., Y. Ma, W. Ma, H. Ishiakawa, F. Sun, S. Ogino, Structural difference of atmospheric

19 boundary layer between dry and rainy seasons over the central Tibetan Plateau (in

20 Chinese),Journal of Glaciology and Geocryology, 33, 72-79, 2011.

21 Lin, W., Xu, X., Zheng, X., Jaxi, D., Ciren, B., Two-year measurements of surface ozone at

22 Dangxiong, a remote highland site in the Tibetan Plateau, J. Environ. Sci., 31, 133-145, 2015.

23 Lüthi, Z.L., Škerlak, B., Kim, S.-W., Lauer, A., Mues, A., Rupakheti, M., and Kang, S.:

24 Atmospheric Brown Clouds reach the Tibetan Plateau by crossing the Himalayas, Atmos.

25 Chem. Phys., 15, 6007-6021, 2015.

26 Ma, J., Liu, H., and Hauglustaine, D.: Summertime tropospheric ozone over China simulated

27 with a regional chemical transport model 1. Model description and evaluation, J. Geophys.

28 Res., 107, ACH 27-21–ACH 27-13, doi:10.1029/2001JD001354, 2002a.

29 Ma, J., Tang, J., Zhou, X., and Zhang, X.: Estimates of the Chemical Budget for Ozone at

30 Waliguan Observatory, J. Atmos. Chem., 41, 21–48, doi:10.1023/A:1013892308983, 2002b.

1 Ma, J., Lin, W. L., Zheng, X.D., Xu, X.B., Li, Z., and Yang, L.L.: Influence of air mass

2 downward transport on the variability of surface ozone at Xianggelila Regional Atmosphere

3 Background Station, southwest China, Atmos. Chem. Phys., 14, 5311–5325, 2014.

4 Ma, Y., Fan, S., Ishikawa, H., Tsukamoto, O., Yao, T., Koike, T., Zuo, H., Hu, Z., and Su, Z.:

5 Diurnal and inter-monthly variation of land surface heat fluxes over the central Tibetan

6 Plateau area, Theoret. Appl. Climat., 80, 259-273, 2005.

7 Ma, W., Ma, Y., and Bob, S.: Feasibility of Retrieving Land Surface Heat Fluxes from

8 ASTER Data Using SEBS: a Case Study from the NamCo Area of the Tibetan Plateau, Arctic,

9 Antarctic, and Alpine Research, 43(2), 239-245, 2011.

10 Ming, J., Du, Z., Xiao, C., Xu, X., and Zhang, D.: Darkening of the mid-Himalaya glaciers

11 since 2000 and the potential causes, Environ. Res. Lett. 7, 014021, doi:10.1088/1748-

12 9326/7/1/014021, 2012.

13 Moore, D.P. and Remedios, J.J.: Seasonality of Peroxyacetyl nitrate (PAN) in the upper

14 troposphere and lower stratosphere using the MIPAS-E instrument, Atmos. Chem. Phys., 10,

15 6117-6128, 10.5194/acp-10-6117-2010, 2010.

16 Myhre, G., Shindell, D., Bréon, F.-M., Collins, W., Fuglestvedt, J., Huang, J., Koch, D.,

17 Lamarque, J.-F., Lee, D., Mendoza, B., Nakajima, T., Robock, A., Stephens, G., Takemura, T.,

18 and Zhang, H.: Anthropogenic and Natural Radiative Forcing. In: Climate Change 2013: The

19 Physical Science Basis. Contribution of Working Group I to the Fifth Assessment Report of

20 the Intergovernmental Panel on Climate Change [Stocker, T.F., D. Qin, G.-K. Plattner, M.

21 Tignor, S.K. Allen, J. Boschung, A. Nauels, Y. Xia, V. Bex and P.M. Midgley (eds.)].

22 Cambridge University Press, Cambridge, United Kingdom and New York, NY, USA, 2013.

23 Ohara,T., Akimoto, H., Kurokawa, J., Horii, N., Yamaji, k., Yan, X., and Hayasaka, T.: An

24 Asian emission inventory of anthropogenic emission sources for the period 1980–2020,

25 Atmos. Chem. Phys., 7, 4419–4444, 2007.

26 Pandey Deolal, S., Staehelin, J., Brunner, D., Cui, J., Steinbacher, M., Zellweger, C., Henne,

27 S., and Vollmer, M. K.: Transport of PAN and NOy from different source regions to the

28 Swiss   high   alpine   site   Jungfraujoch,   Atmos.   Envron.,   64,   103–115,

29 doi:10.1016/j.atmosenv.2012.08.021, 2013.

1 Park, M., Randel, W. J., Gettelman, A., Massie, S. T., and Jiang, J. H.: Transport above the

2 Asian summer monsoon anticyclone inferred from Aura Microwave Limb Sounder tracers, J.

3 Geophys. Res., 112, 10.1029/2006jd008294, 2007.

4 Park, M., Randel, W. J., Emmons, L. K., Bernath, P. F., Walker, K. A., and Boone, C. D.:

5 Chemical isolation in the Asian monsoon anticyclone observed in Atmospheric Chemistry

6 Experiment (ACE-FTS) data, Atmos. Chem. Phys., 8, 757-764, 10.5194/acp-8-757-2008,

7 2008.

8 Park, M., Randel, W. J., Emmons, L. K., and Livesey, N. J.: Transport pathways of carbon

9 monoxide in the Asian summer monsoon diagnosed from Model of Ozone and Related

10 Tracers (MOZART), J. Geophys. Res., 114, D08303-D08313, 10.1029/2008jd010621, 2009.

11 Qu, B., Ming, J., Kang, S.-C., Zhang, G.-S., Li, Y.-W., Li, C.-D., Zhao, S.-Y., Ji, Z.-M., and

12 Cao, J.-J.: The decreasing albedo of the Zhadang glacier on western Nyainqentanglha and the

13 role of light-absorbing impurities, Atmos. Chem. Phys., 14, 11117-11128, doi:10.5194/acp-

14 14-11117-2014, 2014.

15 Ramanathan, V., Ramana, M. V., Roberts, G., Kim, D., Corrigan, C., Chung, C., Winker, D.:

16 Warming trends in Asia amplified by brown clouds solar absorption, Nature, 448, 575–578,

17 2007.

18 Ran, L., Lin, W.L., Deji, Y.Z., La, B., Tsering, P.M., Xu, X.B., and Wang, W.: Surface gas

19 pollutants in Lhasa, a highland city of Tibet: current levels and pollution implications, Atmos.

20 Chem. Phys. 14, 10721–10730, 2014.

21 Randel, W. J., Park, M., Emmons, L., Kinnison, D., Bernath, P., Walker, K. A., Boone, C.,

22 and Pumphrey, H.: Asian Monsoon Transport of Pollution to the Stratosphere, Science

23 Magazine, 328, 611-613, 10.1126/science.1182274, 2010.

24 Remedios, J. J., Allen, G., Waterfall, A. M., Oelhaf, H., Kleinert, A., and Moore1, D. P.:

25 Detection of organic compound signatures in infra-red, limb emission spectra observed by the

26 MIPAS-B2 balloon instrument, Atmos. Chem. Phys., 7, 1599-1613, 10.5194/acp-7-1599-

27 2007, 2007.

28 Roiger, A., Aufmhoff, H., Stock, P., Arnold, F., and Schlager, H.: An aircraft-borne chemical

29 ionization - ion trap mass spectrometer (CI-ITMS) for fast PAN and PPN measurements,

30 Atmos. Meas. Tech., 4, 173-188, 10.5194/amt-4-173-2011, 2011.

1   Roberts, J. M.: PAN and Related Compounds, in: Volatile Organic Compounds in the
2   Atmosphere, edited by: Koppmann,R., Blackwell Publishing, 500, Oxford, UK, 2007.

3   Russo, R. S., Talbot, R. W., Dibb, J. E., Scheuer, E., Seid, G., Jordan, C. E., Fuelberg, H. E.,
4   Sachse, G. W., Avery, M. A., Vay, S. A., Blake, D. R., Blake, N. J., Atlas, E., Fried, A.,
5   Sandholm, S. T., Tan, D., Singh, H. B., Snow, J., and Heikes, B. G.: Chemical composition of
6   Asian continental outflow over the western Pacific: Results from Transport and Chemical
7   Evolution over the Pacific (TRACE-P), J. Geophys. Res., 108, 10.1029/2002jd003184, 2003.

8   Shen, R.-Q., Ding, X., He, Q.-F., Cong, Z.-Y., Yu, Q.-Q., and Wang, X.M.: Seasonal
9   variation of secondary organic aerosol tracers in Central Tibetan Plateau, Atmos. Chem. Phys.,
10 15, 8781-8793, 2015.

11 Singh, H.B.: Reactive nitrogen in the troposphere. Environ. Sci. & Technol., 21(4), 320–327,
12 1987.

13 Singh, H.B., Salas, L., Herlth, D., Kolyer, R., Czech, E., Avery, M., Crawford, J.H., Pierce,
14 R.B., Sachse, G.W., Blake, D.R., Cohen, R. C., Bertram, T.H., Perring, A., Wooldridge, P.J.,
15 Dibb, J., Huey, G., Hudman, R.C., Turquety, S., Emmons, L.K., Flocke, F., Tang, Y.,
16 Carmichael, G.R., and Horowitz, L.W.: Reactive nitrogen distribution and partitioning in the
17 North American troposphere and lowermost stratosphere, J. Geophys. Res., 112, D12S04,
18 doi:10.1029/2006JD007664, 2007.

19 Sudo, K., Takahashi, M., and Akimoto, H.: CHASER: A global chemical model of the
20 troposphere 2. Model results and evaluation, J. Geophys. Res, 107, 4586,
21 doi:10.1029/2001jd001114, 2002.

22 Stull, R.B.: An Introduction to Boundary Layer Meteorology, Kluwer Academic, Dordrecht,
23 The Netherlands, 1988.

24 Talbot, R. W., Dibb, J. E., Scheuer, E. M., Kondo, Y., Koike, M., Singh, H. B., Salas, L. B.,
25 Fukui, Y., Ballenthin, J. O., Meads, R. F., Miller, T. M., Hunton, D. E., Viggiano, A. A.,
26 Blake, D. R., Blake, N. J., Atlas, E., Flocke, F., Jacob, D. J., and Jaegle, L.: Reactive nitrogen
27 budget during the NASA SONEX Mission, Geophys. Res. Lett., 26, 3057-3060,
28 10.1029/1999GL900589, 1999.

29 Talukdar, R. K., Burkholder, J. B., Schmoltner, A.-M., Roberts, J. M., Wilson, R. R., and
30 Ravishankara, A. R.: Investigation of the loss processes for peroxyacetyl nitrate in the

1 atmosphere: UV photolysis and reaction with OH, J. Geophys. Res., 100, 14163–14173,
2 10.1029/95JD00545, 1995.

3 Thakur, A.N., Singh, H.B., Mariani, P., Chen, Y., Wang, Y., Jacob, D.J., Brasseur, G., Müller,
4 J.F., and Lawrence, M.: Distribution of reactive nitrogen species in the remote free
5 troposphere: data and model comparisons, Atmos. Environ., 33, 1403–1422,
6 doi:10.1016/s1352-2310(98)00281-7, 1999.

7 Tereszchuk, K.A., Moore, D.P., Harrison, J.J., Boone, C.D., Park, M., Remedios, J.J., Randel,
8 W.J., and Bernath, P.F.: Observations of peroxyacetyl nitrate (PAN) in the upper troposphere
9 by the Atmospheric Chemistry Experiment-Fourier Transform Spectrometer (ACE-FTS),
10 Atmos. Chem. Phys., 13, 5601-5613, 10.5194/acp-13-5601-2013, 2013.

11 Tian, W., Chipperfield, M., and Huang, Q.: Effects of the Tibetan Plateau on total column
12 ozone distribution, Tellus B, 60, 622-635, 10.1111/j.1600-0889.2008.00338.x, 2008.

13 Ungermann, J., Ern, M., Kaufmann, M., Müller, R., Spang, R., Ploeger, F., Vogel, B., and
14 Riese, M.: Observations of PAN and its confinement in the Asian summer monsoon
15 anticyclone in high spatial resolution, Atmos. Chem. Phys., 16, 8389–8403, 2016.

16 Volz-Thomas, A., Xueref, I., and Schmitt, R.: An automatic gas chromatograph and
17 calibration system for ambient measureme, Environ. Sci. Pollut. Res., 9, 72-76, 2002.

18 von Kuhlmann, R., Lawrence, M.G., Crutzen, P.J., and Rasch, P.J.: A model for studies of
19 tropospheric ozone and nonmethane hydrocarbons: Model evaluation of ozone-related species,
20 J. Geophys. Res, 108, 4729, doi:10.1029/2002jd003348, 2003.

21 Wang, M., Xu, B., Cao, J., Tie, X., Wang, H., Zhang, R., Qian, Y., Rasch, P. J., Zhao, S., Wu,
22 G., Zhao, H., Joswiak, D. R., Li, J., and Xie, Y.: Carbonaceous aerosols recorded in a
23 southeastern Tibetan glacier: analysis of temporal variations and model estimates of sources
24 and radiative forcing, Atmos. Chem. Phys., 15, 1191-1204, doi:10.5194/acp-15-1191-2015,
25 2015.

26 Wang, T., Wong, H.L.A., Tang, J., Ding, A., Wu, W.S., and Zhang, X.C.: On the origin of
27 surface ozone and reactive nitrogen observed at a remote mountain site in the northeastern
28 Qinghai-Tibetan Plateau, western China, J. Geophys. Res., 111, D08303,
29 doi:10.1029/2005JD006527, 2006.

Wang, Q.Y., Gao, R.S., Cao, J.J., Schwarz, J.P., Fahey, D.W., Shen, Z.X., Hu, T.F., Wang, P., Xu, X.B., and Huang, R.J.: Observations of high level of ozone at Qinghai Lake basin in the northeastern Qinghai-Tibetan Plateau, western China, J. Atmos. Chem., 72, 19–26, 2015.

Wiegele, A., Glatthor, N., Höpfner, M., Grabowski, U., Kellmann, S., Linden, A., Stiller, G., and von Clarmann, T.: Global distributions of C_2H_6, C_2H_2, HCN, and PAN retrieved from MIPAS reduced spectral resolution measurements, Atmos. Meas. Tech., 5, 723-734, 10.5194/amt-5-723-2012, 2012.

Worden, J., Jones, D.B.A., Liu, J., Parrington, M., Bowman, K., Stajner, I., Beer, R., Jiang, J., Thouret, V., Kulawik, S., Li, J.-L. F., Verma, S., and Worden, H.: Observed vertical distribution of tropospheric ozone during the Asian summertime monsoon, J. Geophys. Res., 114, D13304-D13320, 10.1029/2008jd010560, 2009.

Xiong, X., Houweling, S., Wei, J., Maddy, E., Sun, F., and Barnet, C.: Methane plume over south Asia during the monsoon season: satellite observation and model simulation, Atmos. Chem. Phys., 9, 783-794, 2009.

Xu, W., Lin, W., Xu, X., Tang, J., Huang, J., Wu, H., and Zhang, X., Long-term trends of surface ozone and its influencing factors at the Mt. Waliguan GAW station, China – Part 1: Overall trends and characteristics, Atmos. Chem. Phys., 16, 6191–6205, 2016.

Xu, W., Xu, X., Lin, M., Lin, W., Tang, J., Tarasick, D., Ma, J., and Zheng, X.: Long-term trends of surface ozone and its influencing factors at the Mt. Waliguan GAW station, China, Part 2: Variation mechanism and links to some climate indices, Atmos. Chem. Phys. Discuss., https://doi.org/10.5194/acp-2017-483, 2017.

Xue, L.K., Wang, T., Zhang, J.M., Zhang, X.C., Deliger, Poon, C.N., Ding, A.J., Zhou, X.H., Wu, W.S., Tang, J., Zhang, Q.Z., and Wang, W.X.: Source of surface ozone and reactive nitrogen speciation at Mount Waliguan in western China: New insights from the 2006 summer study, J. Geophys. Res., 116, 10.1029/2010jd014735, 2011.

Yeh, T.-C., Lo, S.-W., and Chu, P.-C.: The wind structure and heat balance in the lower troposphere over Tibetan Plateau and its surroundings, Acta Meteor. Sinica (in Chinese), 28, 108-121, 1957.

Yin, X., Kang, S., de Foy, B., Cong, Z., Luo, J., Zhang, L., Ma, Y., Zhang, G., Rupakheti, D., and Zhang, Q.: Surface ozone at Nam Co (4730 m a.s.l.) in the inland Tibetan Plateau:

1 variation, synthesis comparison and regional representativeness, Atmos. Chem. Phys.

2 Discuss., https://doi.org/10.5194/acp-2017-175, 2017.

3 Zanis, P., Ganser, A., Zellweger, C., Henne, S., Steinbacher, M., and Staehelin, J.: Seasonal

4 variability of measured ozone production efficiencies in the lower free troposphere of Central

5 Europe, Atmos. Chem. Phys., 7, 223-236, 10.5194/acp-7-223-2007, 2007.

6 Zhang, H., Xu, X., Lin, W., and Wang, Y.: Wintertime peroxyacetyl nitrate (PAN) in the

7 megacity Beijing: Role of photochemical and meteorological processes, J. Environ. Sci., 26,

8 83–96, 10.1016/S1001-0742(13)60384-8, 2014.

9 Zhang, L., Jacob, D.J., Boersma, K.F., Jaffe, D.A., Olson, J.R., Bowman, K.W., Worden, J.R.,

10 Thompson, A.M., Avery, M.A., Cohen, R.C., Dibb, J.E., Flock, F.M., Fuelberg, H.E., Huey,

11 L.G., McMillan, W.W., Singh, H.B., and Weinheimer, A.J.: Transpacific transport of ozone

12 pollution and the effect of recent Asian emission increases on air quality in North America: an

13 integrated analysis using satellite, aircraft, ozonesonde, and surface observations, Atmos.

14 Chem. Phys., 8, 6117–6136, doi:10.5194/acp-8-6117-2008, 2008.

15 Zhang, Q., Streets, D.G., Carmichael, G.R., He, K.B., Huo, H., Kannari, A., Klimont, Z., Park,

16 I.S., Reddy, S., Fu, J.S., Chen, D., Duan, L., Lei, Y., Wang, L.T., Yao, Z.L., Asian emissions

17 in 2006 for the NASA INTEX-B mission, Atmos. Chem. Phys. 9, 5131-5153, 2009.

18 Zhang, R., Wang, H., Qian, Y., Rasch, P. J., Easter, R. C., Ma, P.-L., Singh, B., Huang, J.,

19 and Fu, Q.: Quantifying sources, transport, deposition and radiative forcing of black carbon

20 over the Himalayas and Tibetan Plateau, Atmos. Chem. Phys., 15, 6205–6223, 2015.

21 Zhao, S., Ming, J., Sun, J., and Xiao, C.: Observation of carbonaceous aerosols during 2006–

22 2009 in Nyainqêntanglha Mountains and the implications for glaciers, Environ. Sci. Pollut.

23 Res., DOI 10.1007/s11356-013-1548-6, 2013.

24 Zheng, X. D., Shen, C. D., Wan, G. J., Liu, K. X., Tang, J., and Xu, X. B.: ^{10}Be/^{7}Be implies

25 the contribution of stratosphere-troposphere transport to the winter-spring surface O_3 variation

26 observed on the Tibetan Plateau, Chinese Sci. Bull., 56, 84–88, 2011.

27 Zhou, X., Lou, C., Li, W.L. and Shi, J.E. Ozone changes over China and low center over

28 Tibetan Plateau, Chin. Sci. Bull., 40, 1396–1398, 1995.

1   Zhu, T., Lin, W.L., Song, Y., Cai, X.H., Zou, H., Kang, L., Zhou, L.B., and Akimoto, H.:

2   Downward transport of ozone-rich air near Mt. Everest, Geophys. Res. Lett. 33 (23), L23809,

3   doi: 10.1029/2006GL027726, 2006.

1   Table 1 Concentrations of PAN at different heights above the TP. Data from literature are

2   acquired either through remote sensing method or global modeling, while data from this work

3   are estimates based on analysis of ground measurements.

Average PAN concentration(ppb)	Period	Height	Reference
around 0.5	25 May 2012	~350 hPa	this work
0.6-0.7	22 August 2011	~350 hPa	
0.35-0.45	March 2003	333 hPa	
0.15-0.23		234 hPa	Moore and Remedios (2010)
0.35-0.5	August 2003	278 hPa	
0.15-0.23		185 hPa	
0.1-0.15	October 2007	12km	Wiegele et al.(2012)
0.1-0.2	21 October 2003	12km	Glatthor et al.(2007)
0.30-0.50	June-August 2008	2-6km	Fischer et al.(2014)
0.2-0.4		6-10km	
0.15-0.2	June-September 1995-2004	6-10km	Fadnavis et al. (2014)
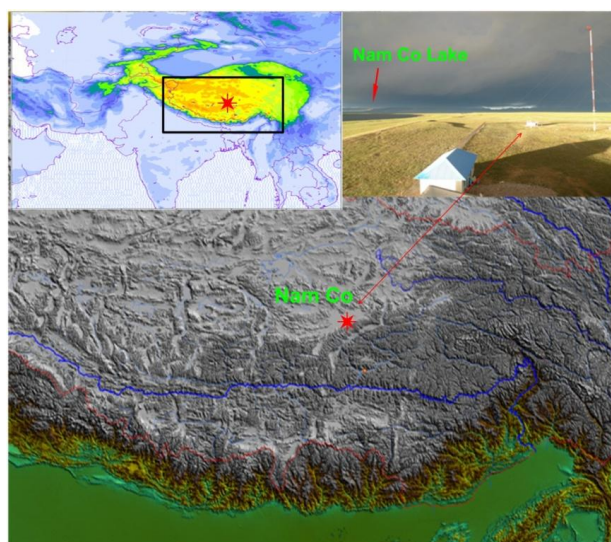
2   Fig.1 Map showing location of the observation site and local environment.
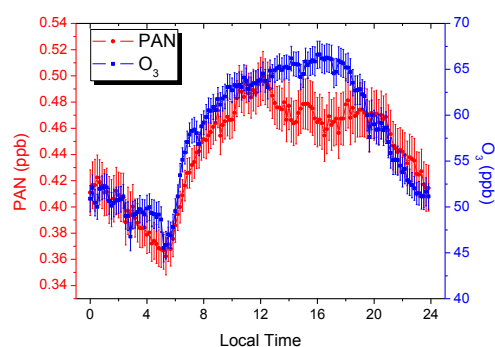
2   Fig.2 Diurnal patterns of PAN and O_3. All data are processed as 10 minutes resolution. The

3   vertical bars represent one standard error of the mean.
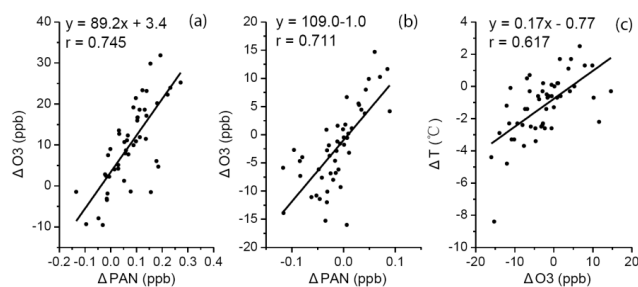
2   Fig.3 Scatter plots of ΔPAN (variation of the PAN concentration), ΔO₃ (variation of the O₃

3   concentration) and ΔT (variation of temperature) in specific time spans: (a) from 5:00 LT to

4   9:00 LT; (b, c) from 2:00 LT to 4:00 LT. All correlations shown in the figures are statistically

5   significant at α=0.01.
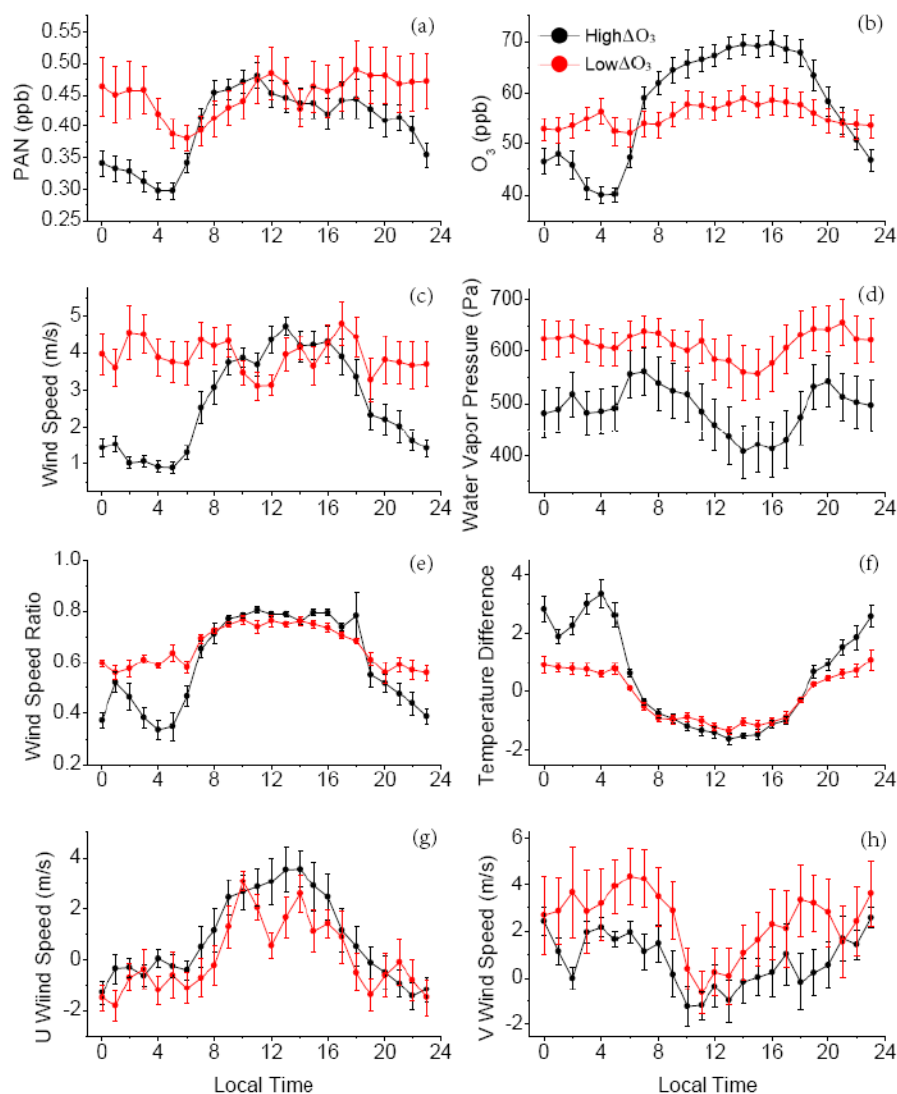
Fig. 4 Diurnal patterns of PAN (a), O_3 (b), Wind Speed (c), Water Vapor Pressure (d), Wind

Speed Ratio (e, ratio of 10 meters height wind speed and 2 meters height wind speed),

Temperature Difference (f, subtraction of 20 meters height temperature and 10 meters height

temperature), U wind speed (g) and V wind speed (h). Black curves represent diurnal curves

of 15 days with greatest ΔO_3 from 7:00 BJT to 11:00 BJT, and red curves represent diurnal

curves of 15 days with smallest ΔO_3 correspondently. The vertical bars represent one standard

error of the mean.
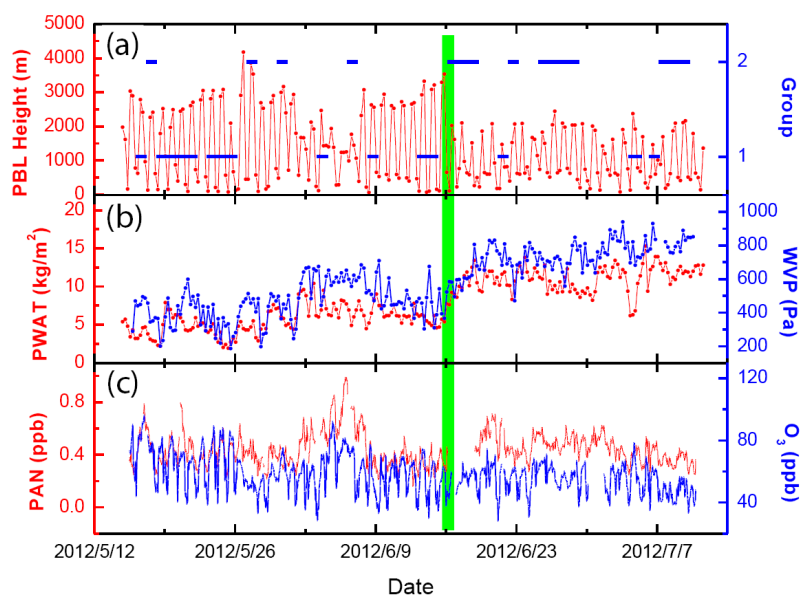
2   Fig. 5 Distribution of two groups of days (classified following Fig. 4) and time series the PBL

3   height, PWAT (Precipitable Water of Entire Atmosphere), WVP (Water Vapor Pressure),

4   PAN and O$_3$. The PBL Height and PWAT are acquired from the FNL data with temporal

5   resolution of 6 hours. WVP are calculated and processed as 6-hours resolution data from field

6   observation. PAN and O$_3$ concentrations are processed as hourly data.
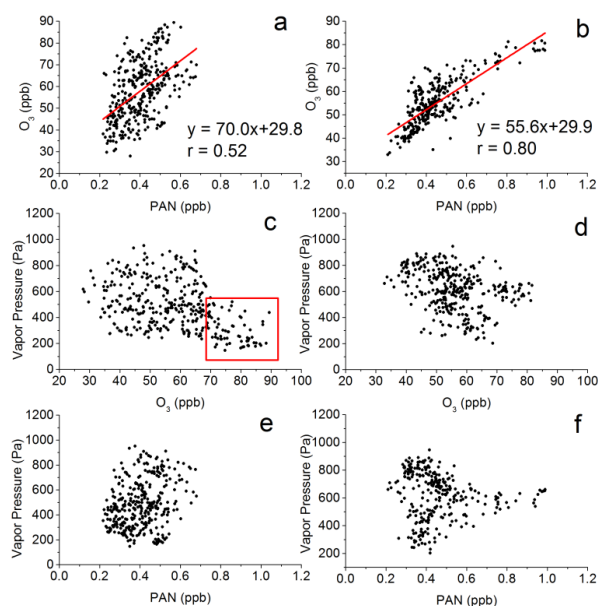
2   Fig. 6 Scatter plots of hourly O_3-PAN, Vapor Pressure- O_3, Vapor Pressure-PAN of group 1

3   (a,c,e) and group 2 (b,d,f), following Fig. 4. The correlation shown in Figs. 6(a) and 6(b) are

4   significant at α=0.01. The data points within the red rectangle in Fig. 6(c) represent O_3 levels

5   higher than 70 ppb and WVP lower than 500 hPa.
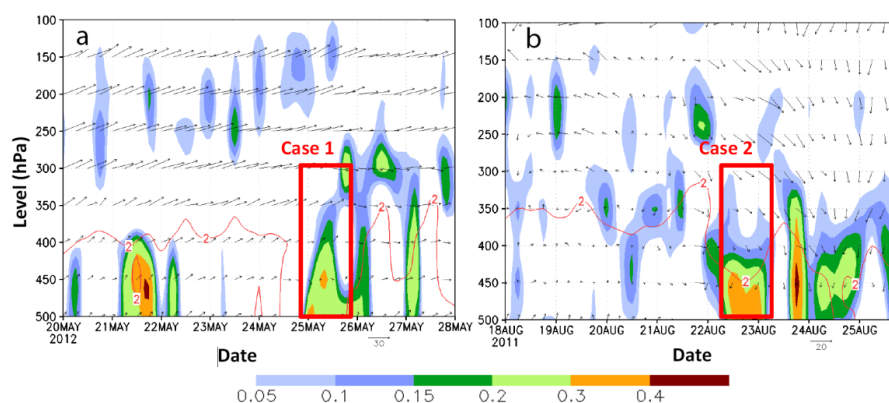
Fig. 7 Omega (shaded), specific humidity (red line) and horizontal wind field in dependence
of time and height in two time frames. (a) From 20 to 28 May 2012; (b) From 15 to 25 August
2011. Case 1 and Case 2 correspond to two significant downdraft events.
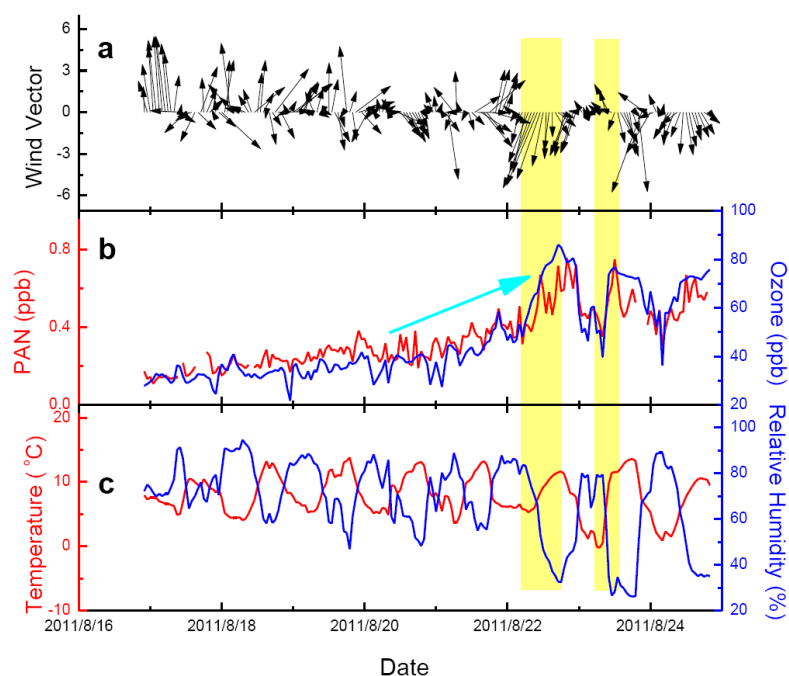
2   Fig. 8 Time series of (a) surface wind vectors, (b) PAN and O₃, and (c) temperature and

3   relative humidity during 16-25 August 2011. Yellow shadows represent the short periods

4   controlled by downward motion. The blue arrow indicates the increasing trend of PAN and O₃.
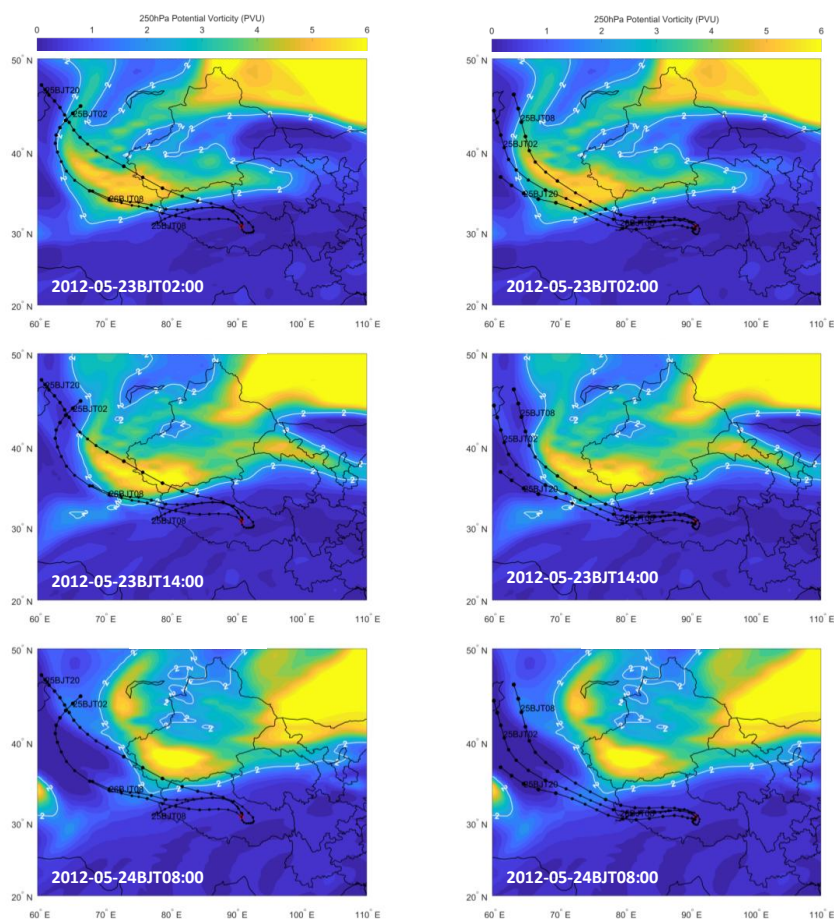
2   Fig. 9 Plots showing 250 hPa potential vorticity fields at three timepoints during 23-24 May

3   2012 and back trajectories of air masses arriving at 500 m (left) and 1500 m (right) above

4   ground of the NMC site (red star) during 25-26 May 2012.
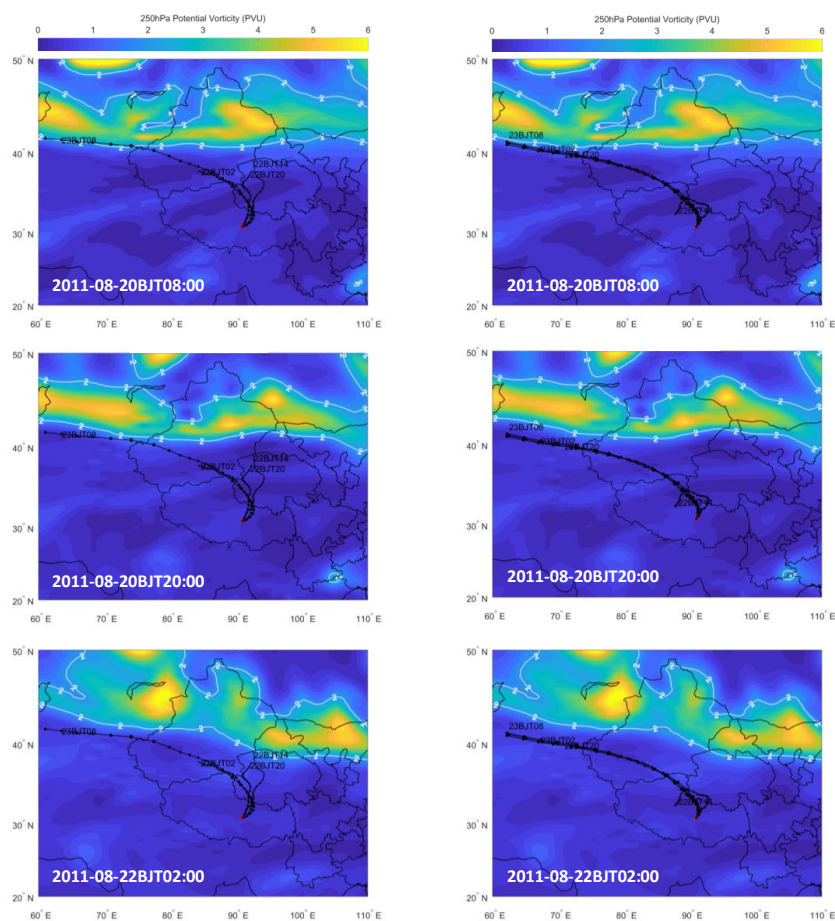
2   Fig. 10 Plots showing 250 hPa potential vorticity fields at three timepoints during 20-22

3   August 2011 and back trajectories of air masses arriving at 500 m (left) and 1500 m (right)

4   above ground of the NMC site (red star) during 22-23 August 2011.
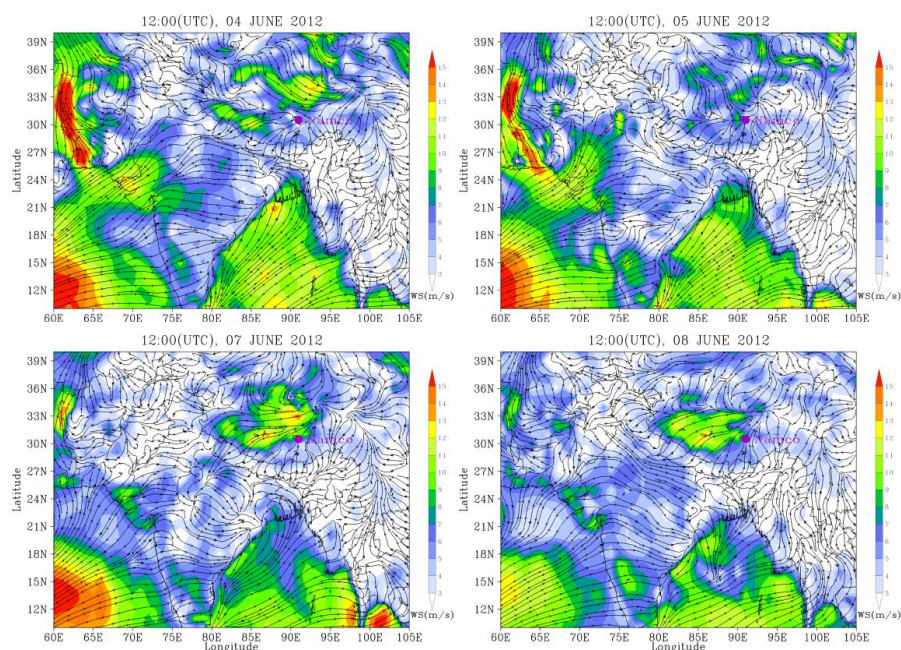
2   Fig. 11 Average fields of wind at sigma=0.995 for 12:00 (UTC) of 4, 5, 7 and 8 June 2012.
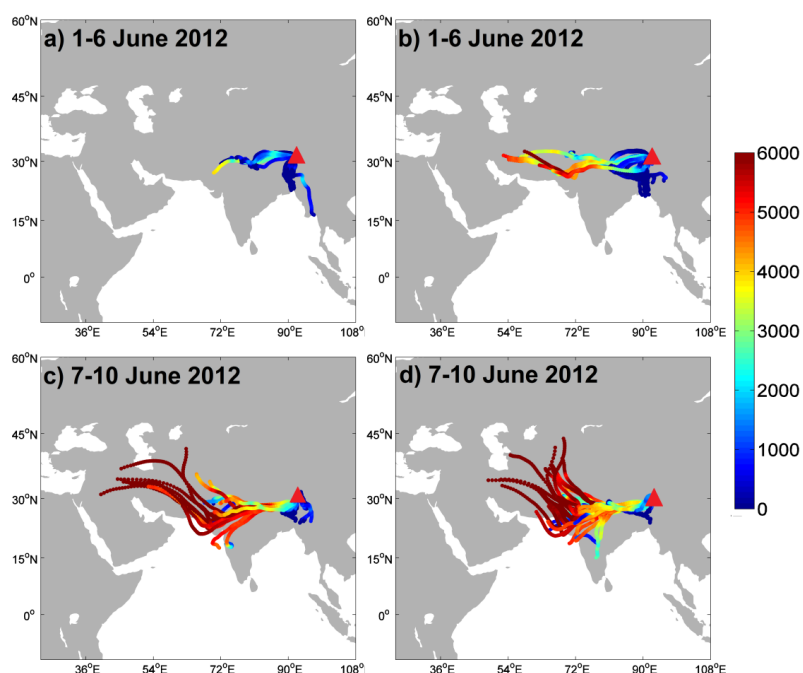
Fig. 12 Backward air trajectories arriving at NMC with endpoint heights of 500 meters (a,c)

1500 meters (b,d) for the periods 1-6 June 2012 (a,b) and 7-10 June 2012 (c,d).